

Experimental evidence for equilibrium surface segregation in a CoPd alloy

Przemysław J. Godowski* and Stefan M. Zuber

Institute of Experimental Physics, University of Wrocław, Pl. Maxa Borna 9, 50-204 Wrocław, Poland. E-mail: pjg@spin.ifd.uni.wroc.pl

Received 9th March 1999, Accepted 2nd June 1999

The surface concentration of a polycrystalline Co–Pd(30 at%) alloy was investigated over a wide temperature range by Auger electron spectroscopy. Reversible changes of surface composition were observed at temperatures of 800–1080 K. Above 1100 K, irreversible depletion of palladium in the surface region occurred. Auger transitions of different energies were used for depth profile characterization. Variation of the palladium concentration with temperature at the surface–bulk equilibrium showed palladium segregation with a heat of segregation of $Q = 27 \text{ kJ mol}^{-1}$.

Introduction

Surface segregation phenomena in binary metallic alloys have been the subject of a large number of studies.^{1,2} In the usual segregation model comprising two phases, the bulk and the surface, the formula for the surface (C^S) to bulk (C^B) concentration is given by eqn. (1):³

$$\frac{C^S}{1-C^S} = \frac{C^B}{1-C^B} \times \exp(Q/RT) \quad (1)$$

where Q is the heat of segregation. As shown in the past, the segregation experiment should ensure the proper experimental arrangement (e.g. ref. 4) and the possibility of analysis of diffusion and evaporation limits among the data (e.g. ref. 5,6). Any conclusion could be drawn on the basis of surface composition data measured in equilibrium conditions as a function of the sample temperature.

Changing the surface composition of cobalt-based alloys has significant consequences in catalysis.^{7–12} The aim of the present paper is to characterize the $\text{Co}_{70}\text{Pd}_{30}$ polycrystalline alloy surface using Auger electron spectroscopy (AES). Studies conducted on polycrystalline samples reveal the average properties of the alloys investigated and certain characteristic quantities, which have more practical significance. The present work is devoted to collecting new results on this Co–Pd alloy, i.e. the temperature range of equilibrium in ultra high vacuum (UHV) conditions, heat of segregation and expected surface content at moderate temperatures.

Experimental

The UHV system, described previously,⁸ was equipped with a new home-made four-grid retarding field analyser of LEED-AES type. The pressure of residual gases in the system after evacuation at around 500 K for 12 h did not exceed 5×10^{-8} Pa. The ingot of the $\text{Co}_{70}\text{Pd}_{30}$ polycrystalline alloy was prepared from high purity powders (Johnson-Matthey Chemicals, Ltd.) by sintering and homogenization in an inert atmosphere (N_2) at around 1550 K over 100 h. X-Ray diffraction analysis of the sample confirmed the homogeneity of the alloy. A specimen slice of 10 mm in diameter and 0.8 mm thick was cut from the roller-shaped ingot and mechanically polished with diamond paste. In order to markedly reduce the contamination level and to obtain a flat surface, the slice was annealed under a hydrogen atmosphere at approximately 750 K for 12 h before mounting. The sample was spot welded to two tungsten wires of 0.4 mm in diameter and about 20 mm

length. This holder allowed sample heating up to high temperatures with negligible distortion of the secondary electron distribution from the sample during Auger measurements.¹³ The temperature of the sample relative to the reference junction at room temperature (RT) was controlled by a Pt–PtRh(10 at%) thermocouple spot welded to the rear side of the sample. The alloy surface was cleaned in UHV by K^+ ion bombardment (500 eV, 10 μA , 750 K) from a zeolite source of simple construction.¹⁴ After K^+ ion bombardment at RT, the Auger spectrum contained a well resolved potassium LMM peak at 252 eV. Additional heating to around 900 K was sufficient for removal of residual potassium from the surface. *Ex situ* reduction in hydrogen effectively removed carbon from the subsurface region as was confirmed by the intensity ratio between the peak near 278 eV and the peak at 330 eV.⁶ After only two series of ion bombardments sulfur and phosphorus peaks appeared. This competitive behaviour of contaminants is characteristic for group VIIIa metal surfaces. It was concluded that sulfur and/or phosphorus surface segregation on the $\text{Co}_{70}\text{Pd}_{30}$ alloy excludes the presence of surface carbon. Sulfur and phosphorus in turn translocates palladium and cobalt atoms, respectively, from the topmost layers. The Auger signal due to phosphorus disappeared after three series of potassium ion bombardments. The bombardment time required for sulfur removal at high temperatures was longer, but not as long as in the cases of the samples not subjected to hydrogen treatment.⁸ After the cleaning procedure, the sample was annealed in UHV up to 750 K for 50 h to remove residual hydrogen and attain equilibrium.

At each selected temperature, the Auger electron spectra (dN/dE) were obtained using a 3 kV electron beam of normal incidence to the investigated sample surface. The spectra were recorded on an XY recorder and/or stored in a PC under modulation voltages chosen according to the energy interval. Extreme care was taken to ensure the stability and reproducibility of the measurements. A typical spectrum obtained during these investigations is shown in Fig. 1. Low kinetic energy Auger transitions of Pd43 and Co53 were clearly resolved and, together with high energy ones (Pd330 and Co775), were suitable for conventional peak height analysis. The modulation voltage in the low energy dN/dE region (not shown in the graph) was reduced in order to obtain a reasonable signal to noise ratio with the background slope as small as possible.

Results

Starting from 750 K, the sample was heated at a given temperature until no changes with time were detected in the

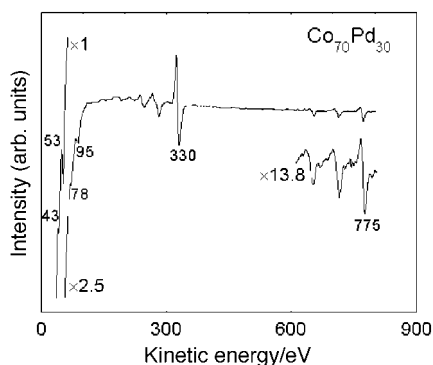


Fig. 1 The dN/dE spectrum of a clean $\text{Co}_{70}\text{Pd}_{30}$ alloy surface at room temperature obtained in the 4-grid retarding field analyzer, LEED-AES type, under a primary electron beam energy of 3 keV. Indicated factors of multiplication include magnification of the signal due to different modulation voltages used at different energy intervals.

Auger spectrum. The following annealing times fulfilled the above requirement: up to 850 K, over 16 h; for the 850–950 K interval, 8 h; for 950–1050 K, 5 h; and above 1050 K, less than 3 h. Results, presented as the ratios of the peak heights, $h_{\text{Pd}43}/h_{\text{Co}53}$ and $h_{\text{Pd}330}/h_{\text{Co}775}$, versus the sample temperature, are collected in Fig. 2. The ratio of low energy peaks decreases approximately linearly with the temperature and near 1080 K drops more rapidly. The dependence is reproducible, within experimental error, up to around 1050 K. This corresponds to a decrease of the palladium concentration in the analyzed volume with temperature, demonstrating the occurrence of Pd surface segregation in the investigated alloy. Heating the sample above 1080 K for around 1 h caused irreproducible reduction of the palladium Auger peak. After annealing the alloy up to 1230 K, the peaks ratio, obtained after the shorter annealing time as above, follow in parallel with the lower values of the ratio, as indicated by the arrow in Fig. 2(a). This is a clear demonstration of how easy it is to get misleading results. Although the high energy region of the Auger spectrum

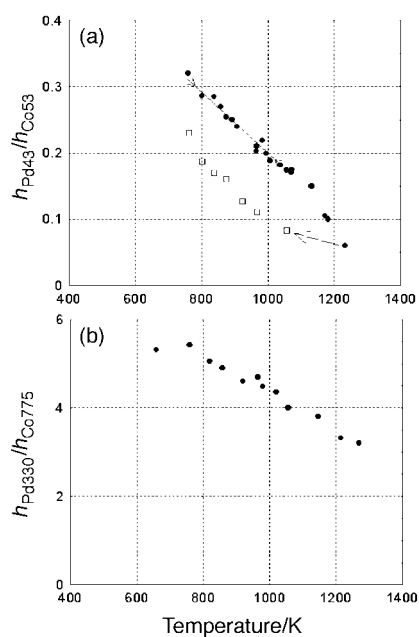


Fig. 2 Auger peak heights ratio as a function of the temperature of the $\text{Co}_{70}\text{Pd}_{30}$ alloy: (a) $h_{\text{Pd}43}/h_{\text{Co}53}$; the line shows the region in which results were reproducible with increasing and decreasing temperature. After heating up to 1230 K, the changes obtained in non-equilibrium conditions follow the points lying under previous results. (b) $h_{\text{Pd}330}/h_{\text{Co}775}$.

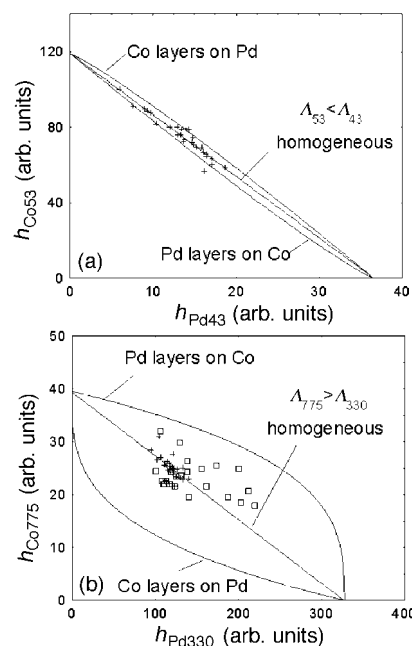


Fig. 3 Plot of the Auger peak height of cobalt as a function of the Auger peak height of palladium: (a) Co MVV 53 eV vs. Pd NVV 43 eV; (b) Co LVV 775 eV vs. Pd MVV 330 eV. The least squares fit to the part of the data (crosses) represented by the straight line on the graph yields the relation between h_{Co}^0 and h_{Pd}^0 . The continuous lines are variations of the Auger signals as calculated from the layer-by-layer growth model. All the data obtained in the experiment should be contained in the region limited by these curves.

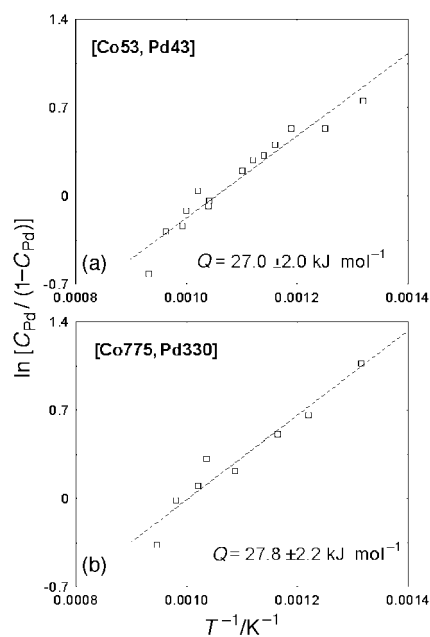


Fig. 4 Arrhenius plot for concentration versus temperature data according to eqn. (1) in the temperature range of 760–1073 K at equilibrium: (a) low energy Auger transitions; (b) high energy Auger transitions. The slope of the straight line determines the heat of Pd segregation in the $\text{Co}_{70}\text{Pd}_{30}$ alloy.

was not so intensively investigated, the results of the $h_{\text{Pd}330}/h_{\text{Co}775}$ Auger peaks ratio of the reproducible temperature–time region, with the exception of the last two points, are shown in Fig. 2(b). The data show similar behaviour with smaller relative changes in the peak ratio.

The surface composition of the alloy can be assessed directly from the Auger signal intensities ratio as follows. For a

Table 1 Values used in Auger quantification. The monolayer thickness, a , and the electron escape depth were calculated according to ref. 15. For the LEED-AES $A=0.74\lambda$, where λ is the attenuation length, given by $\lambda=[(528/E^2)+0.42(aE)^{1/2}]a$, where E denotes kinetic energy of Auger electrons (in eV). The attenuation length, determined from the equation, expresses the intrinsic property of Auger electrons created in the element

Element	Monolayer thickness (a)/nm	Auger transition	Energy of transition/eV	Electron escape depth (A)/nm
Co	0.222	M ₂₃ VV	53	0.268
		L ₂ VV	775	2.15
Pd	0.245	N ₂₃ VV	43	0.300
		M ₅ VV	330	0.685

homogeneous CoPd alloy it may be shown that eqn. (2) holds:¹³

$$C_{Pd}^{av} = \frac{h_{Pd}/h_{Co}}{h_{Pd}/h_{Co} + h_{Pd}^0/h_{Co}^0} \quad (2)$$

where h denotes the peak height of a given Auger transition, the subscript denotes the element and the superscript 0 denotes the value for the pure element. C_{Pd}^{av} is the average palladium concentration in the analyzed volume of the alloy. For small values of the electron escape depths, A , of both Pd and Co Auger transitions (*i.e.* when $A \approx$ the average monolayer thickness), C_{Pd}^{av} is very close to the surface concentration, *i.e.* the concentration of the topmost layer. When the concentration of the first layer differs from that of the other layers having an average bulk composition we have eqn. (3):¹³

$$C_{Pd}^S = \frac{1 - C_{Pd}^B [\exp(-d/A_{Co}) + \frac{h_{Pd}^0/h_{Co}^0}{h_{Pd}/h_{Co}} \exp(-d/A_{Pd})]}{1 - \exp(-d/A_{Co}) + \frac{h_{Pd}^0/h_{Co}^0}{h_{Pd}/h_{Co}} [1 - \exp(-d/A_{Pd})]} \quad (3)$$

where the average monolayer thickness d (in nm) is given by $d = C_{Pd}^B a_{Pd} + C_{Co}^B a_{Co}$ and a is the monolayer thickness (in nm).¹⁵ From eqn. (3) the concentration can be determined, regardless of whether the A and h_{Pd}^0/h_{Co}^0 values are known. The best source for the attenuation length is the compilation of the experimental data.¹⁵ On the basis of the method described in ref. 16, the h_{Pd}^0/h_{Co}^0 ratio was determined from the data recorded during the whole experiment. Using the measured pairs of $\{h_{Pd}, h_{Co}\}$, representing varying compositions, the peak height of h_{Co} plotted against h_{Pd} can be fitted by a straight line intercepting the axes at the h_{Co}^0 and h_{Pd}^0 values. The graphs of $\{h_{Pd43}, h_{Co53}\}$ and $\{h_{Pd330}, h_{Co775}\}$ are shown in Fig. 3. Together with the straight line representing homogeneous alloy, two curves corresponding to uniform films of Co on Pd and Pd on Co for the appropriate electron escape depths are shown. The extent of the curve depends on the relation between the A values as indicated in the figure. All the experimentally determined Auger peak heights should fall inside the domain bounded by the two curves (self-checking method). The $\{h_{Pd43}, h_{Co53}\}$ points follow a straight line within experimental error and the determined ratio of h_{Pd}^0/h_{Co}^0 seems to be a very good approximate value. For $\{h_{Pd330}, h_{Co775}\}$, only selected data lie on a straight line (crosses) and the remaining points (open squares) show inhomogeneous distribution in depth with Pd enrichment.

Using the parameters in Table 1, the surface concentrations of palladium, C_{Pd}^S , and the average concentrations, C_{Pd}^{av} , were calculated. Determined C_{Pd}^S predominates over C_{Pd}^{av} , especially at low temperatures, *i.e.* around 760 K. This property demonstrates the validity of using eqn. (3) in quantifi-

cation. The heat of segregation was evaluated from the data obtained over the temperature range 760–1073 K using eqn. (1). From the slope of the straight line shown in Fig. 4, Q is equal to 27.0 ± 2 kJ mol⁻¹. This value enables us to calculate the equilibrium surface composition of the alloy for any bulk content.

Conclusions

The simple criteria of segregation predict opposite effects for the CoPd alloy. The lower melting point of cobalt (Co, 1768 K; Pd, 1825 K) suggests a greater tendency for Co surface enrichment but its smaller atomic radius (Co, 0.125 nm; Pd, 0.137 nm) implies a greater release of elastic strain energy when a Pd atom is moved to the surface. However, Pd has a lower surface energy (2100 mJ m⁻²) than Co (2550 mJ m⁻²) and hence Pd segregation is expected, as the difference in surface energy should have the largest effect on surface composition. The obtained result, namely the occurrence of palladium segregation in the CoPd alloy, agrees with the predictions of Chelikowsky¹⁷ and Miedema,¹⁸ which are also discussed in a review by Ossi.¹⁹

Acknowledgements

This work was supported by the University of Wrocław under Project No. 2016/W/IFD/97.

References

- 1 W. M. H. Sachtler and R. A. Van Santen, *Appl. Surf. Sci.*, 1979, **3**, 121.
- 2 P. Modrak, *Prog. Surf. Sci.*, 1995, **49**, 227.
- 3 J. Du Plessis and G. N. Van Wyk, *J. Phys. Chem. Solids*, 1988, **49**, 1441.
- 4 M. P. Seah and C. Lea, *Philos. Mag.*, 1975, **31**, 627.
- 5 G. P. Schwartz, *Surf. Sci.*, 1978, **76**, 113.
- 6 J. C. Hamilton and J. M. Blakely, *Surf. Sci.*, 1980, **91**, 199.
- 7 E. E. Hajcsar, P. R. Underhill, W. W. Smeltzer and P. T. Dawson, *Surf. Sci.*, 1987, **191**, 249.
- 8 J. Rudny and P. J. Godowski, *Pol. J. Chem.*, 1987, **61**, 499.
- 9 M. J. Dees and V. Ponc, *J. Catal.*, 1989, **119**, 376.
- 10 P. J. Godowski, *Appl. Surf. Sci.*, 1991, **47**, 333.
- 11 W. Juszczyk, Z. Karpiński, J. Pielaszek and Z. Paal, *J. Catal.*, 1993, **143**, 583.
- 12 A. R. Belambe, R. Oukaci and J. G. Goodwin Jr., *J. Catal.*, 1997, **166**, 8.
- 13 P. J. Godowski and P. Marcus, *Acta Phys. Pol., A*, 1995, **87**, 619.
- 14 P. J. Godowski and S. Mróz, *Thin Solid Films*, 1984, **111**, 129.
- 15 M. P. Seah and W. A. Dench, *Surf. Interface Anal.*, 1979, **1**, 2.
- 16 W. Palmer and K. Röhl, *Surf. Interface Anal.*, 1983, **5**, 105.
- 17 J. R. Chelikowsky, *Surf. Sci.*, 1984, **139**, L197.
- 18 A. R. Miedema, *Z. Metallkol.*, 1978, **69**, 455.
- 19 P. M. Ossi, *Surf. Sci.*, 1988, **201**, L519.